UNIVERSITY OF BUCHAREST
FACULTY OF CHEMISTRY
DOCTORAL SCHOOL IN CHEMISTRY

PhD THESIS
ABSTRACT

Functionalised heterogeneous catalysts for selective and sustainable valorization of lignocellulosic biomass

PhD Student:
ALINA ELENA NEGOI

PhD Supervisor:
Prof. VASILE I. PÂRVULESCU

Doctoral Committee:

President: prof. Camelia BALA

Supervisor: prof. Vasile I. PÂRVULESCU

Official referents:

1. Prof. dr. Ion GROSU, Babeș-Bolyai University, Cluj-Napoca
2. Prof. dr. Csaba PAIZS, Babeș-Bolyai University, Cluj-Napoca
3. Conf. dr. Niculina HĂDADE, Babeș-Bolyai University, Cluj-Napoca

2022

Tabel of content (corresponding to the PhD thesis)

Introduction

Reducing natural resources and demographic growth have resulted of damage to the environment. At the same time, the increase in energy consumption is forcing the reconsideration and redesign of important chemical processes in order to identify more efficient procedures.

In this context, the catalysis is a key element capable of providing alternatives to this issue. Following the principles of green chemistry, catalysis is involved in a multitude of critical areas for sustainable development: energy, materials, various industrial branches having a role in environmental protection, agriculture, etc.. The concept of sustainable development has been transformed into a strategy to find new ways of long-term economic development, without damaging the environment and with benefits on the quality of life. The development of sustainable chemical processes is one of the prerogatives of modern chemistry, aiming at an efficient use of natural resources and a reduction of energy consumption and the minimization of waste [1]. Thus, social, economic and environmental pressure represent causes for identifying solutions that allow their use to be optimised. In addition, in some cases, such as oil, replecement by renewable sources such as biomass is being considered. The implementation of the concept is based on the interactive participation of the three pilars (Figure 1) [2].

Figure 1. *The interdependence between the three pilars of sustainable development.*

The use of catalysts to carry out chemical transformations is now irreplaceable. More than 85% of chemicals are obtained by processes using catalysts in at least one stage of the manufacturing process (Figure 2). The more complex the practical application is, the more it requires the use of catalysts. Thus, pharmaceutical chemistry and the synthesis of fine chemicals use catalysts to the highest degree.

Renewable sources offer significant potential for the addition/replacement of oil. The valorization of biomass requires a different chemistry from that of oil, appropriate to the abundance

of chemical bonds containing oxygen. Under these conditions, the extraction and chimisation of widely usable molecules (currently defined as platform molecules) is a condition of this capitalization that includes the concept of biorefinery. This concept is analogous to the concept of oil refining. The conversion of biomass through biorefinery is expected to produce fuels, energy and chemical intermediates following new, innovative technologies.

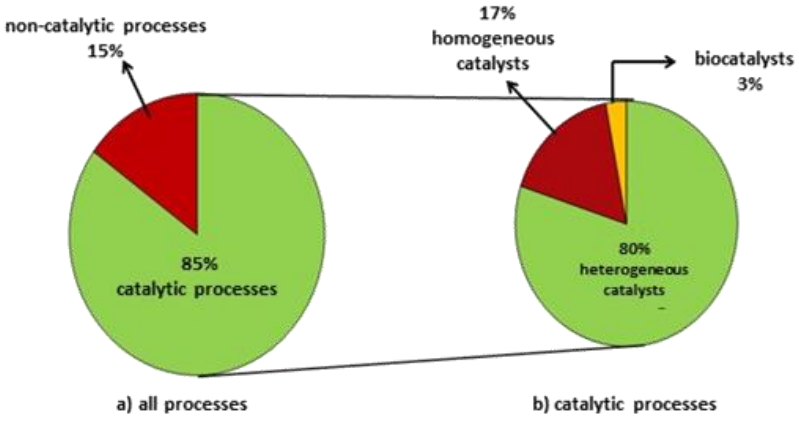

Figure 2. *Use of catalysts in industrial processes.*

Starting from this state of affairs, the first objective of the PhD thesis was to identify new catalysts and investigate their catalytic behaviour in advanced cellulose fragmentation reactions to useful chemicals. The study of the relationship between the structure and the selectivity of the catalyst compared to a particular reaction product was also followed. In particular case of cellulose, its valorisation has been aimed at obtaining added-value chemicals, some of wich served as platform molecules. The fragmentation process of cellulose is relatively difficult due to the complexity of the intra- and inter-molecular hydrogen bonds. Thereby, the rigidity and crystalline nature of cellulose, resulting from intra- and inter-molecular bonds, make it difficult for solvents and catalysts to be accessible to the target bonds.

Acid-catalysed hydrolysis of polysaccharides occurs in a first step by protonation of oxygen from the ether group (Step 1). Protonation is then followed by cleavage of the C-O bond, resulting in the formation of a carbocation and an alcohol (Step 2).

Another major objective of this thesis was to synthesize separable catalysts from solid mixtures and recyclable. The advanced characterization of the synthesized catalysts and the correlation of their properties with activity, selectivity and reaction mechanism were other secondary objectives. The sub-objectives followed in this study were:

i) design of supports with a high specific surface;
ii) control of the dispersion and stability of the active catalytic phase on the surface of the investigated supports;
iii) investigation of metal-support interaction.

The design of separable and recyclable catalysts was achieved by synthesis a magnetic nanosized Fe3O4 core. The stabilisation of the magnetic core was synthesized by encapsulation in

a inert oxide layer of nanometric dimensions. This composite was the support for the heterogeneous catalysts used in these investigations. For comparison, the catalytic performances of other microporous supports, such as zeolites, on whose surface noble metals have been deposited, were also investigated.

A series of nanoscopic materials have been also synthesised to expand the porfolio of acid catalysts for the fast and selective hydrolysis of biomass to glucose. They were pepared by the *sol-gel fluorolysis* method used as a synthetic platform for obtaining nanoscopic catalytic materials with different acid-base properties and for the preparation of bifunctional catalysts. Doping of hydroxylated nanoscopic fluorines prepared with noble metals led to multifunctional fluorinated catalytic systems in which an acidic function was combined with a hydrogenation function.

The deposition of metals (Ru, Rh, Ir, Pd) on these supports was achieved using conventional methods such as dry impregnation, co-precipitation or deposition-precipitation.

Catalytic fragmentation reactions of cellulose were carried out in heterogeneous systems, in liquid phase, both in the presence of molecular hydrogen and by generating it *in-situ* during the process. Metal – support interaction has been demonstrated using characterization techniques such as: XRD, XPS, FTIR, TEM, temperature programmed reduction (TPR), UV-Vis spectroscopy and Mössbauer spectroscopy.

Chapter 1. Valorization of biomass-based green chemistry principles

The literature study presented in Chapter 1 aimed, on one hand, to define the concepts used during the thesis and, on the other hand, to analyse the trends related to the valorisation of biomass into useful products and cellulose fragmentation reactions for the production of platform molecules. The main focus was on lignocellulosic biomass incorporated in plant waste, mainly agricultural.

Green chemistry plays a key role in sustainable development, being structured around environmentally friendly processes with a low negative impact on the environment. Biomass has always been an important source of food, energy, building materials, medicines and value-added chemicals [3]. Lignocellulosic biomass has a complex structure dependent on the source. Compositionally it is formatted of cellulose (38-50%), hemicellulose (23-32%) and lignin (15-25%), and in smaller proportions of pectin, proteins, extracts and ash [4].

Today, several processes and technologies are already available to convert biomass into value-added products. These processes include both physical or mechanical processes, thermochemicals procesess, chemical processes and biological or biochemical processes [5].

Chapter 2. Design of advanced catalytic systems for the selective lignocellulosic biomass upgrading to biochemicals

Chapter 2 presents a literature rewiev on the methods of fragmentation and hydrolysis of cellulose into valuable products, and experimental methods of investigation. In this chapter, new ways of assessing the competitiveness and efficient measures associated with lower energy

consumption, but at the same time more efficient, clean technologies, preventive management, minimisation of non-recyclable waste, environmentally friendly agricultural parctices, etc.. In this context, catalysis is a key element capable of providing alternatives to this issue.

In recent years, biomass conversion processes [6] and the development of new technologies for the production of energy and chemicals from sustainable sources has confirmed the value of biomass as an ideal alternative to fossil resources [7, 8] through the use of carbohydrates, triglycerides and lignocellulose [9].

Cellulose is the most abundant, renewable source of non-edible biomass. Its structure associates with low reactivity has limited an efficient use, with except in papermaking. However, cellulose can be transformed into a variety of chemicals through various catalytic reaction processes suc as hydrogenation, dehydration, hydrolysis, etc. . This has been confirmed by the selective conversion of cellulose, resulting in a wide range of platform molecules such as acids [10, 11], hydroxymethyl-furfural (hmf) [12, 13] or bioethanol [14, 15].

The O/C ratio in lignocellulosic feedstocks is usually higher than in basic chemicals. Therefore, hydrogenolysis of the C-O bond present in polyols and acids is an important reaction [16-19] and in the same time a difficult step in the fragmentation of lignocellulosic biomass [9]. Cellulose deconstruction is strongly affected by the degree of polymerisation, a step that depends on the pretreatment applied (Figure 3). Thus, under acidic or basic conditions, the degree of polymerization of cellulose can be reduced by 86% and 20% respectively [20].

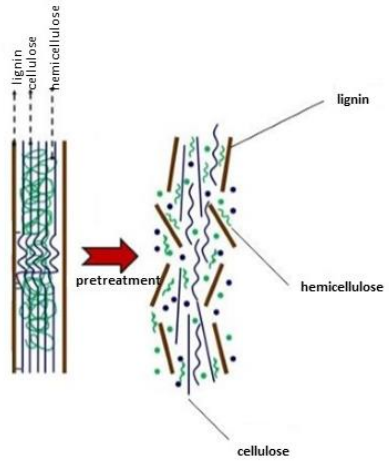

Figure 3. *Pretreatment of lignocellulosic biomass [14].*

Hydrolysis is an alternative route for the transformation of lignocellulosic biomass with selective production of chemical intermediates or hydrocarbons under relatively mild reaction conditions due to the use of catalysts. This also allows selectivity control [21]. Hydrolysis involves cleavage of β (1,4)-glycosidic bonds (Scheme 1). The rigidity and crystalline nature of cellulose, due to strong intra- and inter-molecular hydrogen bonds, make it difficult for solvents and catalysts to access these bonds, thus leading to low yields in glucose and hydrolysis products, respectively [22, 23].

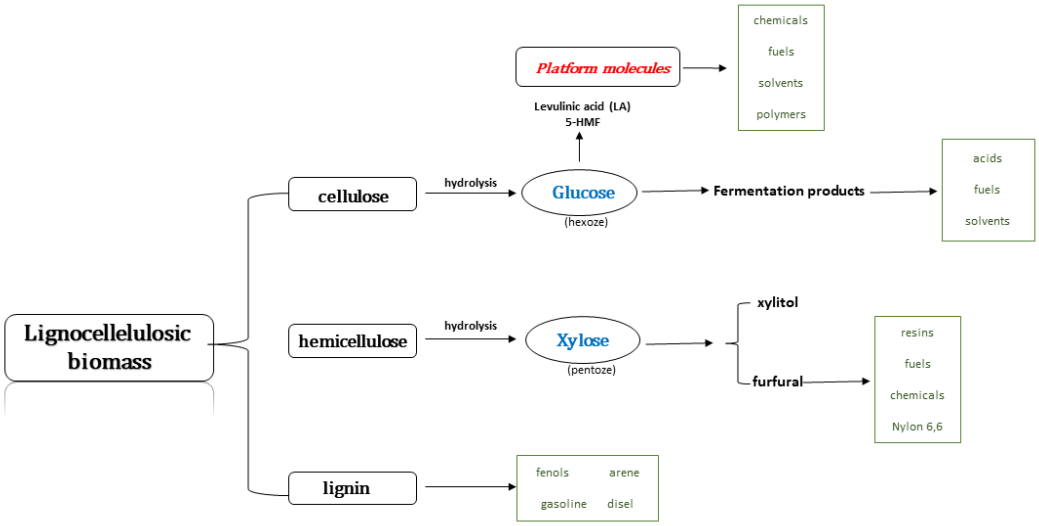

Scheme 1. *The valorization of lignicellulosc biomass.*

A number of heterogeneous catalysts have already been developed for accelerating cellulose depolymerization under hydrothermal conditions and subsequent hydrogenolysis and/or hydrogenation processes [24]. Catalytic conversion of large organic molecules requires catalysts with large pores (mesoporous materials) that can accommodate bulky materials. Their association with tungsten-based catalytic structures in combination with reducible transition metals has led to reliable materials with high selectivity and catalytic activity [25], capable of catalyze the hydrogenation of glucose to sorbitol and the hydrogenolysis of glycerol [26, 27]. The systems containing naonocatalysts have also been effective in hydrogenation, oxidation,C-C coupling, or hydrogenolysis reactions. The same systems have been investigated for biofuel production [28].

Chapter 3. Sn-Doped hydroxylated MgF_2 catalysts for the fast and selective saccharification of cellulose to glucose

Chapter 3 is dedicated to the investigation of tin-doped nanoscopic hydroxylated fluoride-type catalysts in the transformation reaction of cellulose to glucose as an intermediate for the bioethanol production. A series of Sn-doped nanoscopic MgF_2 catalytic samples were synthesized by the *sol-gel fluorolytic* method using a previously reported protocol [29]. They were characterised by specific surface area measurements, XRD, Mössbauer spectroscopy. As secondary objectives the study of the influence of different reaction parameters (temperature, time, etc.) and the influence of Sn concentration were also aimed. The chemical properties of these materials were improved by a modification of the Lewis acidity.

The precursor for Sn was SnF_4, in concentrations of 1, 5, 10, 15, and 20% metal respectively. The synthesis of the magnesium fluoride support (MgF_2) has been carried out in two steps:

i) reaction of the magnesium methoxide with a stoichiometric amount of nonaqueous HF solution in methanol (n<2);

ii) step followed by the addition of the stoichiometrically required amount of water, followed by calcination at 350ºC for 3h in an Ar atmosphere.

The prepared catalysts are referred to hereafter, for simplification, as MgF_2-y%SnF_4: MgF_2-1%SnF_4, MgF_2-5%SnF_4, MgF_2-10%SnF_4, MgF_2-15%SnF_4, and MgF_2-20%SnF_4, indicating the different amounts of SnF_4 used. For comparison, pure hydroxylated MgF_2 and SnF_4 were also prepared and tested.

X-ray diffraction (XRD) results revealed that the crystallinity of the samples changed when going from pure SnF_4 over Sn doped MgF_2 towards pure MgF_2. MgF_2 samples doped with low amounts of SnF_4 not only showed reflexes of both binary metal fluorides, crystalline SnF_4 and weakly crystalline MgF_2, but also additional reflections of a new phase that could not be indexed based on the powder diffraction file (PDF) data bank (Figure 4). Moreover, the diffractogramms of samples MgF_2-1%SnF_4 and MgF_2-5%SnF_4 obviously contain so far an un-known minor crystalline phase that either disappears or at least becomes X-ray amorphous with increasing SnF_4-content.

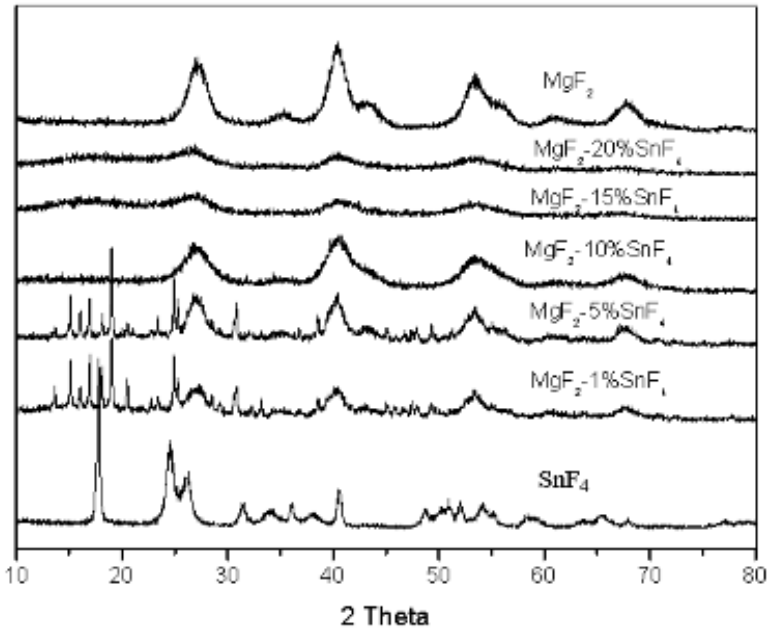

Figure 4. *XRD difractogrames of the Sn-doped magnesium fluorides.*

However, reflections of SnF_4 si MgF_2 totally disappeared at SnF_4 concentrations of 10% and higher. In conclusion, X-ray diffraction (XRD) showed a very high degree of disorder inside the ternary Sn–Mg–F system, which is in line with the observed increase of the surface area (from 143 $m^2 \cdot g^{-1}$ for MgF_2-1%SnF_4 to 221 $m^2 \cdot g^{-1}$ for MgF_2-20%SnF_4) and mesoporosity (pores with diameter of 2.2–3.3 nm). This result is somewhat surprising because the ionic radii of Mg^{2+} (68 pm) and Sn^{4+} (83 pm) are similar.

Nanoscopic hydroxylated MgF_2 was practically inactive for the degradation of cellulose, showing that its medium to strong Lewis/Brønsted acidity is too weak for this reaction (Table 1, entry 1). By contrast, pure nanoscopic hydroxylated SnF_4 showed a high activity, the conversion of cellulose being almost 99% after only 2 h with a selectivity to glucose of 53.6% (Table 1, entry 7).

Table 1. Selected results in the dehydration of cellulose to d-glucose in the presence of the MgF2-y%SnF4 catalysts.

Entry	Catalyst	$C_{cellulose}$ (%)	$\eta_{glucose}$ (%)	$S_{glucose}$ (%)
1[b]	-	12.4	6.5	52.4
2	MgF_2	<10.0-	-	-
3	MgF_2-1%SnF_4	16.0	10.6	66.2
4	MgF_2-5%SnF_4	37.0	29.4	79.4
5	MgF_2-10%SnF_4	40.0	34.9	87.2
6[c]	MgF_2-10%SnF_4	39.2	35.1	89.5
7	MgF_2-15%SnF_4	48.0	33.4	69.6
8	MgF_2-20%SnF_4	59.2	37.4	63.2
9[c]	MgF_2-20%SnF_4	54.4	32.1	59.0
10	SnF_4	98.7	52.9	53.6

[a] Reaction conditions: 0.06 g cat.; 0.14 g cellulose, 8 mL water, 453 K, 2 h; 1100 rpm. [b] 4 h. [c] Recycled catalyst. Note: during each catalyst test the autogenic pressure was 4 atm, demonstrating not all the water evaporated and the reaction took place in liquid aqueous phase.

To explain the obtained results some additional test were performed by keeping the catalyst in water at 453 K, for 2 h under stirring and periodically measuring the pH changes. Indeed, the pH of the catalyst–water slurry went into the acidic domain in the first 30 min (e.g., pH5.6 for MgF_2-10%SnF_4 and pH3.9 for MgF_2-20%SnF_4), and then remained constant for the entire time period investigated. After separation of the catalyst from the aqueous slurry, cellulose was added and kept under reaction conditions similar to those used for catalytic tests. Indeed, the observed modification of the pH was due to the leaching of part of the SnF_4 from the solid catalysts by hydrolysis.

UV/vis characterization confirmed the dissolution of tin fluoride species for the samples with >10% SnF_4. Loadings lower than 10% SnF_4 correspond to stable Sn doped hydroxylated MgF_2 catalysts in which tin is well incorporated in the hydroxylated fluoride matrix. On the contrary, higher loadings of SnF_4 are less stable leading to Brønsted-acidic species in the reaction medium. They were released by the solid material, catalyzing the partial hydrolysis of cellulose to oligomers (e.g., cellobiose, cellotriose, cellotetraose) small enough to penetrate the pore system of the solid and, thus, reach the catalytic active sites.

Analysis of the catalytic samples by Mössbauer spectroscopy coupled with X-ray photoelectron spectroscopy (XPS) also provided an explanation of the different behaviors of the catalysts. Low amounts of SnF_4 obviously formed a kind of (unknown) magnesium fluorostannate

phase that either became amorphous or its formation was suppressed at higher SnF_4 contents (Figure 5).

However, the formation of this phase agrees very well with the XRD analysis results showing an increase of the disorder. The XPS measurements confirmed that the higher the tin concentration, the higher the probability that SnF_4 particles agglomerate and can not be incorporated in the MgF_2 network.

Nevertheless, even in these conditions the obtained yield in glucose (35%) in the presence of the hydrothermally stable MgF_2-10%SnF_4 sample is close to the best results claimed in literature. That is, in the presence of sulfonated activated carbon around 40% yield in glucose was achieved at 423 K) [30].

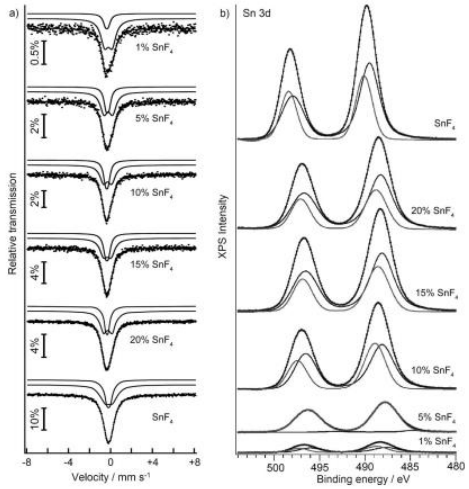

Figure 5. *a) Room-temperaturee Mössbauer spectra for the samples with different concentrations of SnF_4. Source:$^{119}Sn(BaSnO_3)$. b) XPS spectra for Sn3d.*

The synthesized Sn-doped hydroxylated MgF_2 catalysts are very active for cellulose degradation and highly selective to glucose. The cellulose degradation takes place following a two-step homogeneous/heterogeneous mechanism in which an initial partial hydrolysis of cellulose proceeds, involving hydrated tin fluorides released by the solid material in the reaction medium (e.g., for >10% SnF4) or under the effect of harsh reaction conditions (for <10% SnF4). Subsequently, the formed oligomers are small enough to access the pore system where they interact with the active species of the solid catalyst, with formation of glucose.

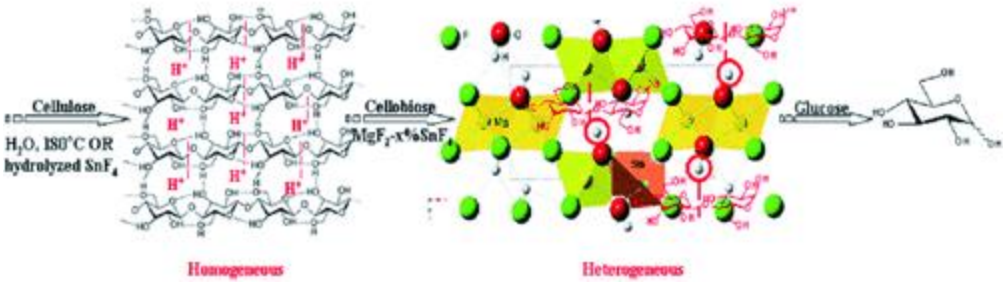

Scheme 1. *Proposed mechanism of cellulose degradation to glucose in the presence of tin-doped hydroxylated MgF_2 catalysts.*

Chapter 4. Direct Synthesis of Sorbitol and Glycerol from Cellulose over Ionic Ru/Magnetite Nanoparticles in the Absence of External Hydrogen

Chapter 4 describes the design of solid Ru-based catalysts deposited on magnetic nanoparticles with high activity and selectivity over homologous homogeneous catalysts. These catalysts exhibited separation properties from the reaction medium and recycling properties for efficient conversion of cellulose to sorbitol. In this study, we aimed to design a cationic Ru-based catalyst deposited on magnetic nanoparticles coated with amino-functionalized silica (Ru/MNP). This catalytic system provided active ionic catalytic centers for a three-step chemical process: 1) selective cellulose dehydration; 2) formic acid decomposition; and 3) hydrogenation of glucose to sorbitol. Levulinic acid aqueous phase reforming (APR) and the water-gas shift (WGS) reaction to form hydrogen and CO_2 are not excluded.

Synthesis of the catalysts was achieved by coating magnetic nanoparticles with silica in a microemulsion. Functionalization of the silica layer with amino groups was achieved using 3-aminopropyltriethoxysilane (APTES). The resulting nano-composite was impregnated with Ru^{III} metal species to generate active centers for catalytic hydrogenation (Scheme 2). The support of functionalized magnetic nanoparticles conferred the necessary properties to catalyze in aqueous medium, reactions demanding acidity, stability and insolubility.

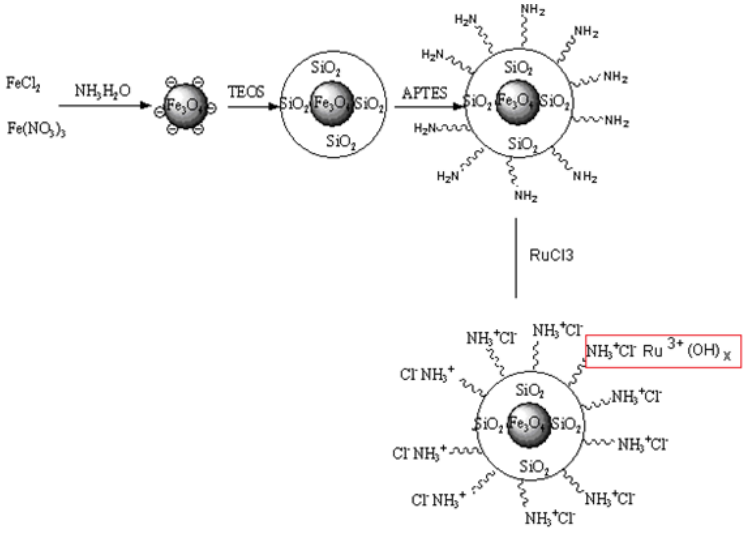

Scheme 2. *Catalyst preparation flow a) Preparation of Si-NPM magnetic particles, b) impregnation of Si-NMP with $RuCl_3$.*

The obtained Ru/MNPs were exhaustively characterized by using nitrogen adsorption–desorption isotherms, XRD, TEM, Mössbauer spectroscopy, magnetic measurements, UV/Vis spectroscopy, extended X-ray absorption fine structure (EXAFS) spectroscopy, and diffuse reflectance infrared Fourier transform (DRIFT) spectroscopy. The Ru/MNPs were then tested as a catalyst for the hydrolysis of cellulose and optimise orking conditions was tested under different temperature, pressure and time conditions. Identification of iron-oxide phases in the iron-oxide–

silica mixture was possible from the XRD patterns, which showed characteristics of a dominant magnetite phase, since both magnetite and maghemite have a spinel structure (Figure 6). The broad diffraction peak at around 2θ 20° is due to the amorphous silica shell on the surface of the magnetite nanoparticles. No hematite (α-Fe_2O_3) or goethite (α-FeOOH) has been identified in these patterns. The crystallite size was approximately of 18 nm for both samples indicating the ruthenium doking of MNP particles did not caused a growth of the particles. Indeed, after the impregnation of ruthenium, no characteristic diffraction planes corresponding to any compound of this metal were identified, indicating a very well dispersion on the magnetic nanoparticles surface (Figure 6).

The presence of the Fe_3O_4 magnetic phase was also confirmed by Mössbauer measurements. In the case of nanoparticles, local configurations with iron defects confirm differences between the particle core and the surface, which corresponds to a rather broad distribution in the Mössbauer spectrum at low temperatures.

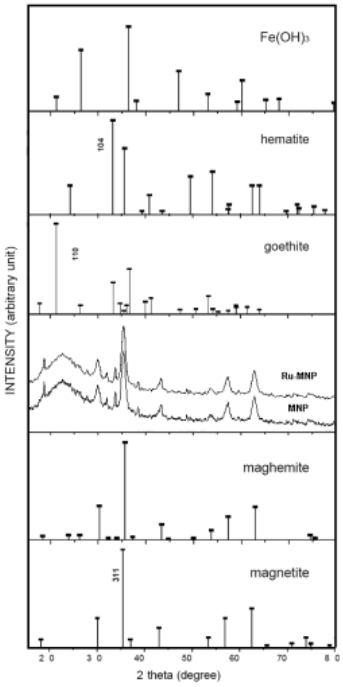

Figure 6. *XRD patterns of MNP (A) and Ru-MNP (B) particles and patterns of oxides and oxyhydroxides from the JCPDS-ICDD database.*

TEM microscopy (Figure 7) demonstrated that the Ru/MNP particles exhibited a discrete uniform core–shell texture with a very narrow size distribution and an average diameter of 22 nm. Together with the XRD results, it was assumed that the difference of 4 nm corresponded to the silica shell thickness.

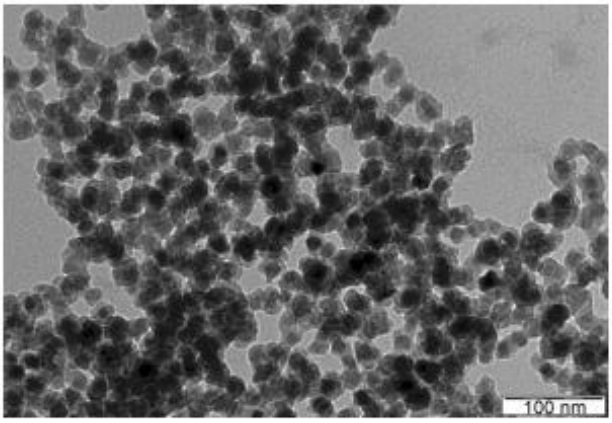

Figure 7. *TEM image of MNP sample.*

UV/Vis time-dependent analysis of the $RuCl_3$ aqueous solution during the ruthenium impregnation, at pH 13, demonstrated the formation of $Ru(OH)_xCl_{3-x}$ species, which is in accordance with previous results presented in Figure 8 [31]. These species further interact with the amino groups of the nanoparticles on which they are docked.

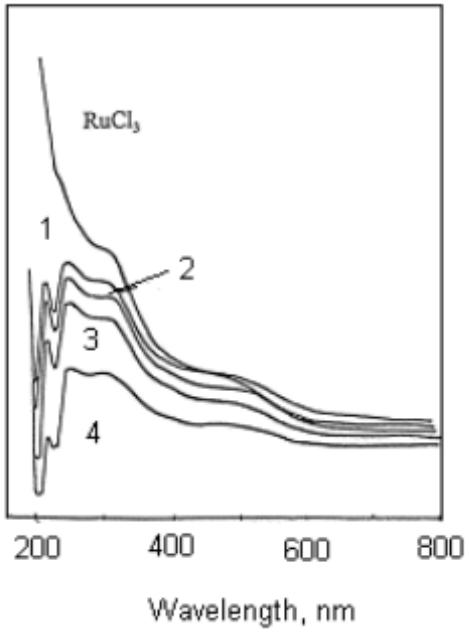

Figure 8. *The evolution in time of the UV-Vis spectra of the $RuCl_3$-base system (1) after 1h, (2) after 2h, (3) after 5h, and (4) after 24h.*

The results are in agree with XRD and EXAFS measurements which shown a stability of the Ru - Cl bond in ruthenium-formed species. Most likely, ruthenium species are anchored to the Si-MNP surface via remnant chloride, which is explained by DRIFT analysis showing the appearance of a new band at 1860 cm^{-1} which was assigned to the $-C-NH_3^+Cl^-$ species (Figure 9).

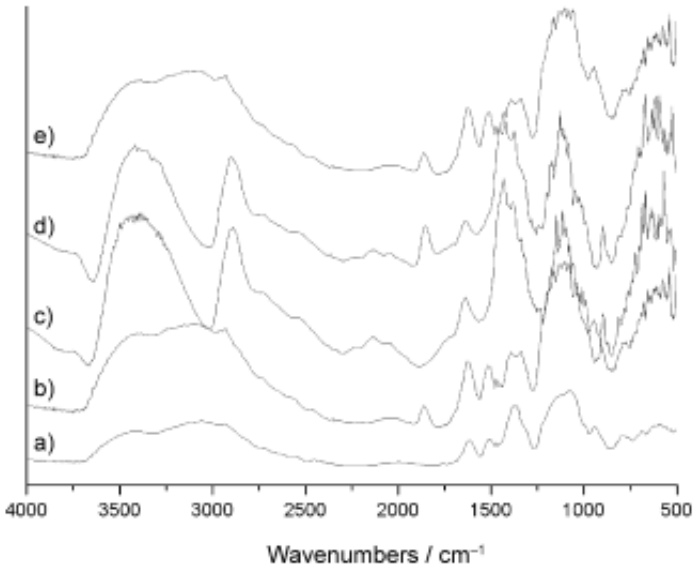

Figure 9. *The DRIFT spectra for a) MNPs, b) Ru/MNPs, c) fresh cellulose, d) Ru/MNPs that had been separated from the supernatant, and e) recovered Ru/MNPs that had been washed three times with distilled water.*

In addition, EXAFS spectra confirmed the existence of a small number of ions in the vicinity of ruthenium.

Catalytic performance (Table 2) did not show any changes after catalyst recycling (Table 2, line 4 and 5), also confirmed by DRIFT analysis (Figure 9, Spectra c,d and e).

Table 2. Cellulose fragmentation in the presence of Ru/MNPs catalyst.

Entry. [a]	**Cellulose conversion (%)**	**η sorbitol[b] (%)**	**η glicerol[c] (%)**	**η xilitol[b] (%)**	**η lichid (%)**	**E_c (%)**
1[c]	33.3	3.2 (13.4)	20.2 (84)	0.6 (2.6)	24.0	72.0
2[d]	14.8	6.9 (64.3)	1.85 (17.7)	1.9 (18.0)	10.65	71.9
3	67.3	3.3 (6.8)	44.4 (91.5)	0.8 (1.7)	48.5	72.1
4[e]	66.7	3.5 (7.2)	43.7 (90.7)	1.0 (2.1)	48.2	72.2

[a] Ru/MNPs catalyst (0.06 g), cellulose (0.14 g), water (5 mL), 453 K, 2 h, 1.200 rpm. [b] Values in parentheses show the product selectivity in the liquid phase;[c] 423 K; [d] 1 h. [e] Recycled catalyst from entry 3.

Table 2 shows the interesting results of cellulose degradation in the presence of the Ru/MNP catalyst. The hydrolysis of cellulose to oligomers is promoted under hot compressed water, in which H_3O^+ species exist, without adding a catalyst [32]. Ru species catalyze the hydrolysis of β-1,4-glycosidic bonds in soluble cellobiose [33]. It is also possible that part of the Ru species generated H^+, via $[Ru(H_2O)_5OH]^{2+}$ as strong Brønsted acids (pKa=2.9 at 298 K). This process takes place in the presence of water, following a similar mechanism that has been reported

by Bottcher et al. for $[Ru(H_2O)_6OH]^{3+}$ [34]. All of these features led to great acceleration of cellulose hydrolysis (Table 2).

To elucidate the formation of sorbitol and glycerol, we performed catalytic tests by using glucose as the raw material and in the presence of prepared catalyst, or of homogeneous $RuCl_3$ and formic acid (Table 3). The Ru/MNPs displayed a close conversion level of glucose with homogeneous $RuCl_3$ species (entries 3 and 4). Moreover, the results obtained clearly show that the ruthenium species were able to decompose the formic acid, either added or formed, during the glucose decomposition.

Table 3. Glucose transformation and selectivities (S) in the presence of formic acid.

Entry [a]	Glucose conversion (%)	$S_{sorbitol}$ (%)	$S_{glicerol}$ (%)	Cyclic isomers	$S_{by\ products}$ (%) LA	Mannitol
1[b]	8.6	1.5	-	64.8	-	-
2[c]	82.0	48.6	15.6	28.6	7.2	-
3	95.4	16.4	66.4	-	-	17.2
4[d]	91.0	27.6	60.8	11.6	-	-

[a] RuCl3 (0.06 g), glucose (0.14 g), water (5 mL), formic acid (0.5 mL), 453 K, 2 h, 1.200 rpm. [b] Blank reaction. [c] No formic acid. [d] Ru/MNPs catalyst.

The Ru/MNPs catalyst also displayed a promotional effect on the hydrolysis of β -1,4-glycosidic bonds. The generated hydrogen was activated by the same ruthenium species, and participated in the consecutive glucose hydrogenation to sorbitol and glycerol (Scheme 3).

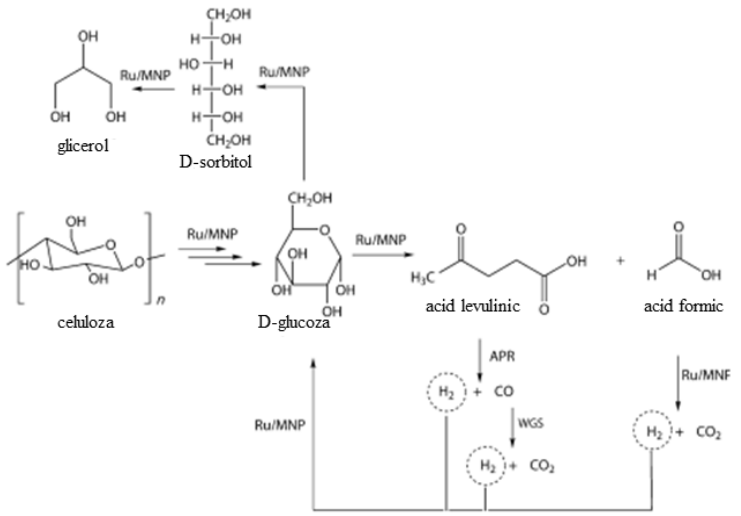

Scheme 3. *Transformation of cellulose into sorbitol and glycerol in the presence of a Ru/MNPs catalyst.*

In conclusion, this contribution reports for the first time the one-pot production of sorbitol and glycerol, starting from cellulose and in the absence of an external hydrogen source. Hydrogen that is produced *in situ* can then be further used for the hydrogenation of glucose to sorbitol and glycerol.

Chapter 5. Cellulose transformation into bio-cemicals in the presence of heterogeneous catalysts

Chapter 5 discusses the catalytic performance of a series of iridium catalysts with different mass concentrations (1-5% Ir) deposited on BEA zeolite in the hydrolytic hydrogenation of cellulose to sorbitol. Catalysts containing other noble metals such as Rh, Ru and Pd were also tested for comparison. The synthesized catalysts were characterized by different textural and morphological techniques. The results of this study demonstrated that regardless of nature of the raw material (glucose or cellulose), the selectivity to sorbitol was parallel to the d-band width of the metal, i.e. Ir > Ru > Rh > Pd. Ru-BEA zeolite is also an efficient catalyst for the direct conversion of cellulose into sorbitol in aqueous media. Besides the metal nature, both the acidic functional groups of BEA zeolite and the high concentration of adsorbed hydrogen species on zeolite surfaces play key roles in sorbitol formation. Moreover, the conversion of cellulose and yield to sorbitol can be greatly improved by adding pure nanoscopic hydroxylated SnF_4 to the catalytic system. Unfortunately, this material is not hydrothermal stable.

X-ray diffraction of catalytic samples showed that the dispersion of these metals is different. In the case of Pd and Pt samples, during catalytic activation a sintering process of the metal on the surface of the support takes place, with the formation of metal particles larger than 5 nm; iridium, ruthenium and rhodium based samples are characterized by a higher dispersion, the diffractograms do not show any line characteristic of the metals [35]. It should be noted that the disappearance of some diffraction lines characteristic of the zeolitic structure after deposition of the metal precursor and catalytic activation indicates a structural change during preparation.

This observation is in line with the TEM measurements that indicated that the active metal species are highly dispersed over the zeolite support, exposing small particles with sizes between 6 and 10 nm (Figure 10).

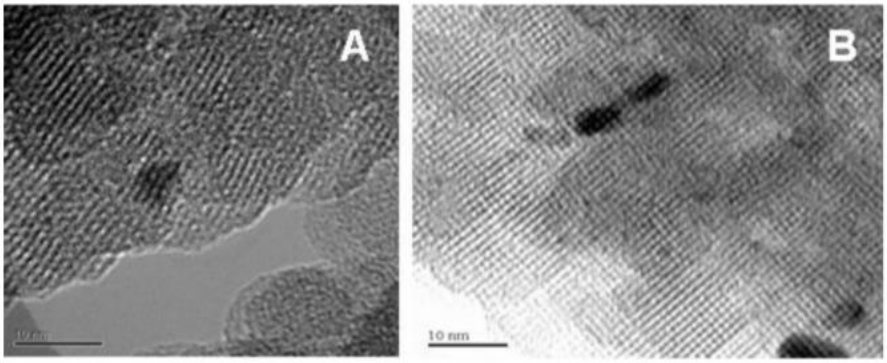

Figure 10. *TEM images of catalysts: (A) 1%Ir/BEA; (B) 3%Ir/BEA.*

Figure 11 presents the O_2-TPO and H_2 -TPR profiles of catalysts with different iridium content synthesized by dry impregnation. The increase of the Ir loading has as an effect the decrease of the temperature at which takes place the reduction of all the species (Figure 11A). This increase corresponds to the decrease of dispersion, which can be correlated with the increase of reduced particle diameter and specific surface area. Based on these results it can be considered that iridium particles interact strongly with the support at lower concentrations. The high dispersion was also confirmed by XRD analysis, which could not identify the presence of reduced iridium regardless of the iridium mass content. In agree with X-ray diffraction, TEM analysis of these samples confirmed a high degree of iridium dispersion on these catalysts. O_2-TPO profiles confirmed the data obtained by H_2-TPR.

Indeed, as H_2-chemisorption measurements showed, depending on the loading of iridium the reduction degree of the supported metal was different. The deposition of iridium on the zeolitic support had the effect of increasing the volume of chemosorbed hydrogen. Moreover, the increase of the iridium content led to a decrease of the dispersion, which actually paralleled the pore blockage observed from the N_2-adsorption–desorption isotherms.

The deconvolution of the XPS bands indicated, indeed, the existence of two species (i.e. reduced and oxidized metal species) irrespective of the metal loading [36]. As expected, the comparison of the analytical and XPS atomic M/Si ratios suggested a relative agglomeration of the metal at the surface. The higher ratios determined for Pd are in a good concordance to the XRD and physisorption measurements. The increase of the metal loading also led to the increase of the M/Si ratios.

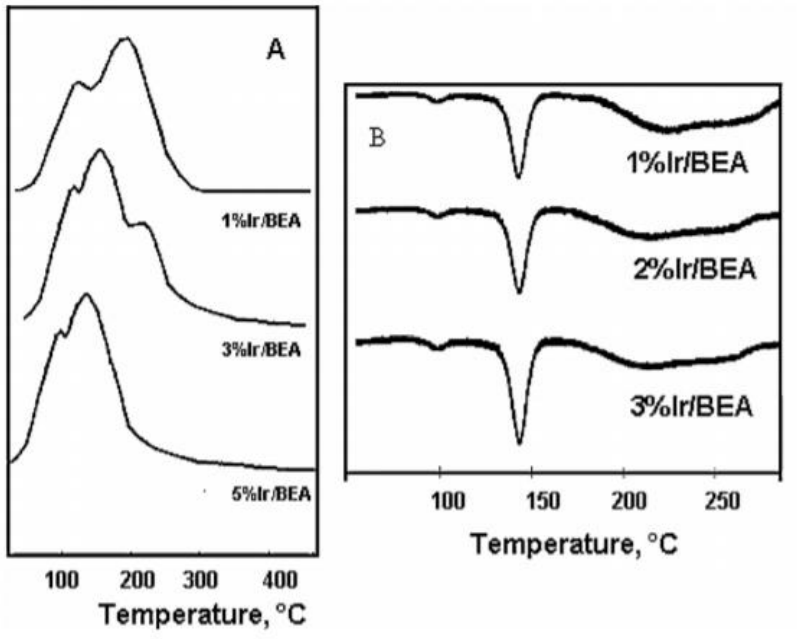

Figure 11. *H_2-TPR (A) and O_2-TPO (B) profiles of Ir-BEA catalysts.*

Figure 12 summarizes the results obtained in the glucose hydrogenation to sorbitol, on all prepared samples. The conversion of glucose paralleled the amount of iridium while the selectivity to sorbitol registered a maximum value for the 3 wt%Ir sample, paralleling the Ir^0/Ir^{n+} ratio.

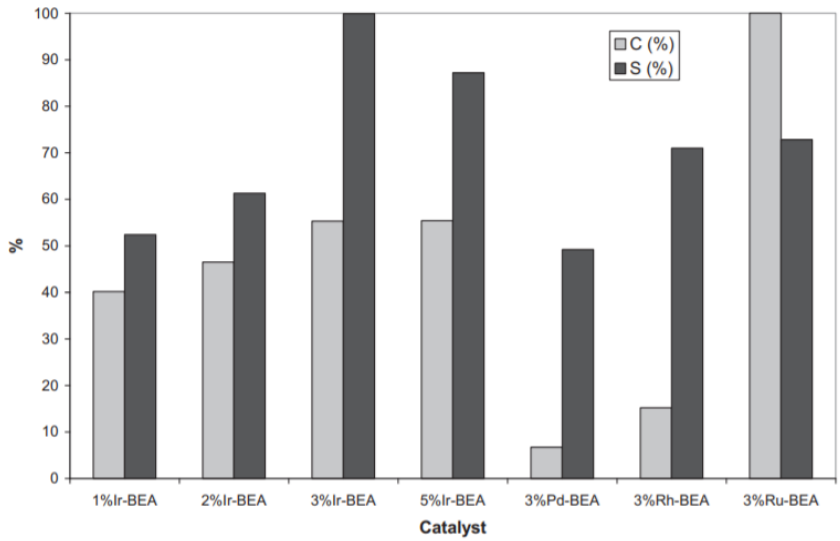

Figure 12. *The variation of conversion and selctivity of glucose to sorbitol as a function of the nature of the metal (reaction conditions: 0.06 g catalyst, 0.14 g glucose, 5 ml water, 16 atm H2, 180 ºC, 3h, 110 rpm [37].*

The hydrogenation reaction was strongly influenced by the metal nature, the highest selectivity in sorbitol being obtained in the presence of 3 wt%Ir-BEA catalyst, followed by Ru and Rh-based catalysts and Pd-based catalyst. The selectivity did not parallel the activity of the catalysts: the highest conversion was obtained on Ru-BEA, followed by 3 wt%Ir-BEA. However, an interesting direct correlation between the d-band width of the metal and the selective hydrogenation was found in the present study: to the wider d-band corresponds the higher selectivity in sorbitol (Figure 12). The increase of the reaction time led to a decrease of the selectivity to sorbitol and the formation of large amounts of 1,4-sorbitan and C-C and/or C-O dissociated compounds such as ethylene glycol and propylene glycol.

As known, the hydrolysis of cellulose takes place even in the absence of any catalytic species, under the effect of harsh reaction conditions (Figure 13). Adding H-BEA zeolite, the conversion of cellulose increased with few percents while the selectivity to glucose decreased. These results suggest a partial hydrolysis of cellulose to oligomers (e.g., cellobiose, cellotriose, cellotetraose, etc.) small enough to penetrate the pore system of the solid and, thus, to reach the catalytic active sites. Nevertheless, once formed, a longer presence in the harsh reaction conditions seems to favor the glucose decomposition to smaller molecules, thus decreasing the selectivity.

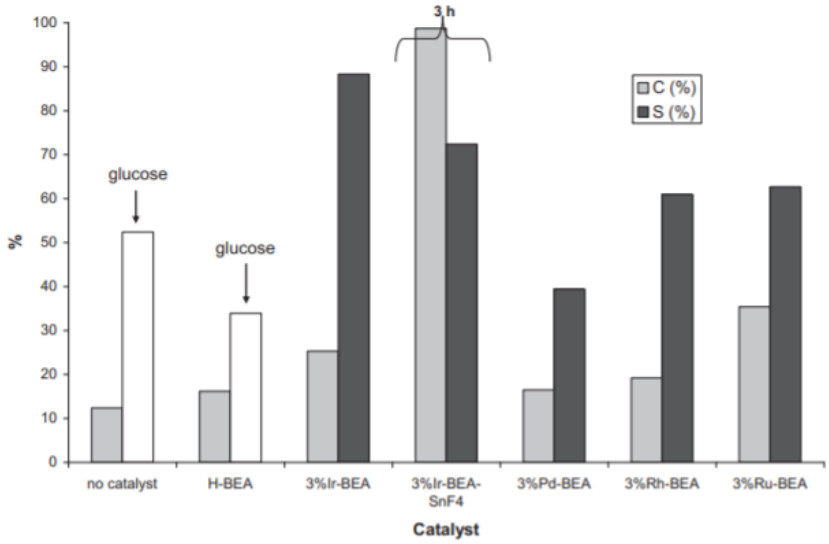

Figure 13. *The variation of the cellulose conversion and the selectivity to sorbitol as a function of the metal nature (reaction conditions: 0.06 g cat.; 0.14 g cellulose, 5 mL water, 16 atm H2, 180 ◦C, 24 h, 1.100 rpm).*

Not long ago we shown the pure nanoscopic hydroxylated SnF_4 and the Sn-doped hydroxylated MgF_2 are very active for the cellulose degradation and highly selective to glucose [38]. Indeed, by adding pure nanoscopic hydroxylated SnF4 to the 3 wt%Ir-BEA (1:1 wt ratio) catalyst, the hydrolysis rate of cellulose was improved (the conversion of cellulose greatly increased till almost 99% after only 3 h) with selectivity to sorbitol of 72.4%. Nevertheless, part of the formed glucose was faster decomposed under harsh reaction conditions, decreasing in this way the selectivity to sorbitol.

The kinetic studies in the hydrolytic hydrogenation of cellulose by supported metal catalysts indicated that metals promote both hydrolysis and hydrogenation steps [39, 40]. Indeed, although in a different proportion, all the investigated metals increased the cellulose conversion by comparison with the cellulose conversion in the presence of BEA zeolite (Figure 13).

In the same chapter, the synthesis of γ-valerolactone (GVL) and methyl-tetrahydrofuran (2-Me-THF) as value-added products from levulinic acid (a platform molecule obtained by cellulose dehydration) in the presence of Ru(0)/Si-MNP (magnetic nanoparticles encapsulated in silica functionalized with propyl amine groups) catalysts was investigated. The deposition of ruthenium species on magnetic nanoparticles aimed to mimic homogeneous catalysts with separation properties from the reaction medium and recycling. Catalytic tests confirmed the activity in the conversion of levulinic acid to gamma-valerolactone. The synthesis of Me-THF request for a bifunctional (acid-reducing) catalyst, the dehydration step of gamma-valerolactone to 1,4-pentanediol requiring a more pronounced acidity than that of silica.

Ru-based magnetic nanoparticle catalysts (Ru^{III}/MNP) showed high activity and selectivity to glucose, were hydrothermally stable and easy to recover and recycle.

The results obtained for the catalytic hydrolysis of cellulose are summarised in Table 4. In the absence of the catalyst, the conversion of cellulose was 10.4 % and small amounts of glucose were detected indicating that hot compressed water can hydrolyze cellulose. This is in accordance

to precedent findings [43]. It is worth to notice that the MNP support did not shown catalytic activity. Over the Ru^{III}/MNP catalyst, the carbon yield of glucose was 8.8 % and selectivity of 84.6 % for a conversion of cellulose of 18.7 % (Table 4, run 3). Both the cellulose conversion (X) and the carbon efficiency (Ec) in liquid phase drastically decreased by comparison with the values obtained in the presence of the Ru^{III}/MNP-NH_2 catalyst. Indeed, taking into account that in the presence of Ru^{III}/MNP-NH_2 catalyst, the acidity of the liquid medium could be increased by the presence of dissolved CO_2 into water, favoring the cellulose hydrolysis [44].

Table 4. Cellulose transformation in the presence of synthesized catalysts.

Entry	Catalyst	$C_{cellolose}$ (%)	$\eta_{glucose}$ (%)	$\eta_{sorbitol}$ (%)	$\eta_{glycerol}$ (%)	$\eta_{xylitol}$ (%)	η_{liquid} (%)	E_C (%)
1[a]	-	10.4	1.6 (22.2)	-	-	-	7.2	69.2
2[b]	Ru^0/MNP	67.3	-	3.3 (6.8)	44.4 (91.5)	0.8 (1.7)	48.5	72.1
3[c]	Ru^{III}/MNP-NH_2	18.7	8.8 (84.6)	-	-	-	10.4	55.6
4[d]	Ru^{III}/MNP	18.2	8.6 (84.3)	-	-	-	10.2	56.0

Reaction conditions: 0.06 g catalyst, 0.14 g cellulose, 5 mL water, 180°C, 2 h, 1,200 rpm. In brackets are given selectivities of the products in liquid phase. [a] Blank reaction, 24h, the carbon yield in glucose isomers was 5.6 %, for a selectivity of 77.8 %; [b] Ref. [45]; [c] The carbon yield in glucose isomers was 1.6 %, for a selectivity of 15.6 %; [d] Recycled catalyst.

The catalyst/product(s) separation was easily achieved with a permanent magnet while the recovered catalyst was reused without a significant loss of the catalytic performances (Table 4). Before recycling, the Ru^{III}/MNP was washed several times in order to totally remove the untransformed cellulose. As DRIFT spectra shown, after three times washing with distilled water, Ru^{III}/MNP was totally cleaned and recovered without loosing the Ru based active catalytic sites (Figure 14).

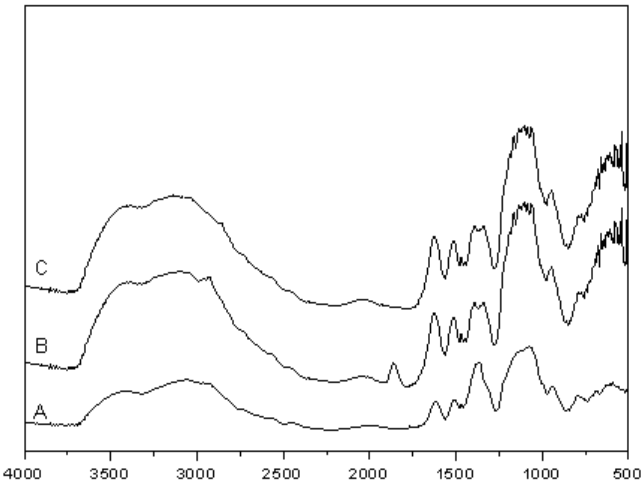

***Figure 14**. DRIFT spectra of fresh cellulose (a), MNP-RuIII separated from supernatant (b), MNP-RuIII washed three times with distilled water (c).*

The same catalysts were also tested in the hydrogenation reaction of levulinic acid (Scheme 4). The most important results are summarized in Table 6 confirming the performance of the heterogeneous catalytic system after chemical reduction of Ru^{III}/MNP with $NaBH_4$.

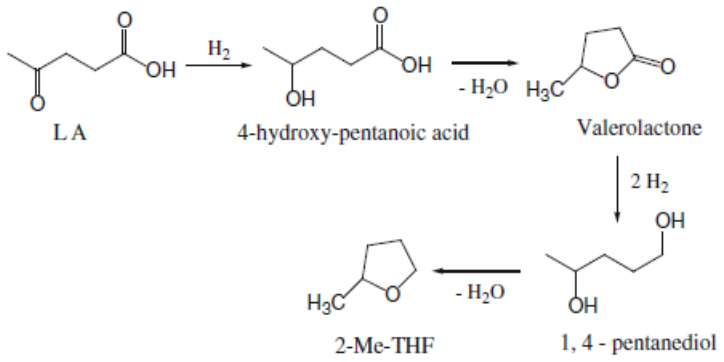

Scheme 4. *The LA reduction to GVL and 2-Me-THF.*

As Table 5 shows, the catalyst displays a high activity (LA conversions of 90–98 %) with a total selectivity to GVL. The synthesis of gamma-valerolactone and Me-THF involves a series of consecutive hydrogenation and dehydration reactions.

Table 5. Catalytic performances of Ru^0/MNP catalyst for the LA reduction

Entry	P_{H2}, (atm)	Reaction time, (h)	C, (%)	S, (%)	
				GVL	By products
1	20	3h	90.0	100	0
2		6h	92.0	100	0
3		12h	92.4	100	0
4		24h	92.5	100	0
5	40	3h	92.3	69.7	30.3
6		6h	93.0	77.6	22.4
7		12h	94.4	100	0
8		24h	98.0	100	0

Reaction conditions: 0.14 g LA, 0.06 g catalyst, water:EtOH = 1:1, 180°C, 1.200 rpm

The catalyst performs its hydrogenation function by generating ruthenium species on the surface of the silica layer which covers the magnetic particles. It should be noted that similar selectivities were also obtained in the presence of the unreduced Ru^{III}/MNP catalyst. This behaviour can be explained through the *in situ* reduction of this catalyst due to the reaction conditions, thus giving an important advantage to the process. Thus, the pre-reduction step can be eliminated using $NaBH_4$. In addition, in the presence of this catalyst the LA conversion is higher than that obtained in the presence of the reduced catalyst, Ru^0/MNP, probably due to the presence of H^+ species (via $[Ru(H_2O)_5OH]^{2+}$) corresponding to strong Brønsted acids [46].

As Table 6 shows on Ru-based catalysts, 2-Me-THF was not generated in detectable amounts. On the contrary, the Ru/BEA zeolite led especially to 2-Me-THF, thus indicating the presence of stronger acid sites. Indeed, zeolites are, by definition, materials with stronger acidity than silica (Scheme 4).

Table 6. Catalytic performances of synthesized catalysts for LA reduction.

Entry	Catalyst	Conversion (%)	S, (%)		
			HPA	GVL	2-MeTHF
1	Ru^0/MNP	90	-	>99	-
2	Ru^{III}/MNP-NH_2	100	>99	-	-
3	Ru^{III}MNP	100	-	>99	-
4	Ru/BEA	15	-	-	97.4

During the catalyst activation (i.e., calcination and reduction in a hydrogen flow and at high temperatures) new protons can be generated enhancing the general acidity of the catalyst [47]. In the presence of Ru/BEA catalysts the conversion of LA was much lower by comparison with that on the other catalysts and this can be due to the mass transport limitations imposed by the microporous structure of zeolites.

The conversion of LA to various C5-oxygenates as HPA, GVL anf 2-Me-THF can also be achieved by selecting the proper catalyst, which could provide a renewable platform for the chemical industry. As a function of the catalyst preparation or the catalyst support, LA can be successfully converted with total selectivity in HPA, GVL or 2-Me-THF. Very important, the unreduced Ru^{III}/MNP catalyst also displays a high selectivity in the LA reduction to GVL and even a higher activity as compared with the Ru^0/MNP catalyst. This remarkable result together with the high activity to the cellulose dehydration made us confident for the development of a one-pot transformation of cellulose into added-value chemicals.

Chapter 6. Catalytic methods for the transformation of marine polysaccharides into monosaccharides and levulinic acid

The Chapter 6 presents results in the development and evaluation of a methodology for the economic and environmental exploitation of *Ulva rigida* marine species, which are an abundant source of biomass along marine coasts. The focus of this study was on the valorisation of marine biomass - *Ulva rigida* in the following directions: (1) catalytic conversion of glucose to levulinic acid; (2) catalytic degradation of cellulose to glucose and levulinic acid; (3) catalytic conversion of polysaccharides extracted from *Ulva rigida* to monosaccharides and levulinic acid. Biomass-derived catalysts (Starbons®) have acid-induced properties. Also, the surface and textural properties as well as the type and strength of the acid centres can be controlled by the calcination and drying temperatures of the triflic acid treated materials.

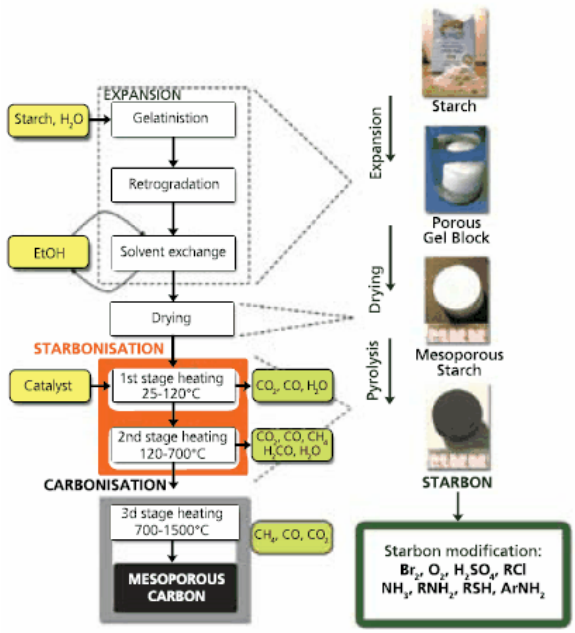

Schema 4. *Synthesis of Starbon.*

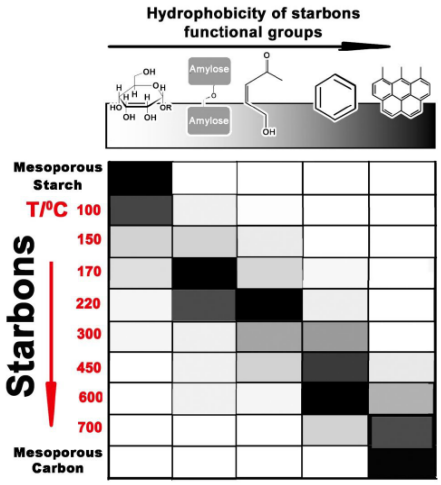

Scheme 5. *Variation of hydrophobicity function of treatment temperature.*

Starbon synthesis valorizes the ability of the amylose and amylopectin polymer chains in the starch structure to self-assemble into large, organized, mesoporous structures. The Starbon® synthesis method comprises of three key stages. Firstly, corn starch is gelatinised by heating in water for 48 h and subsequently cooled to 5°C for one to two days to yield a porous gel block. The water in the block is then exchanged with ethanol and oven dried to yield a predominantly mesoporous starch with a surface area of 180 m^2/g. In the final stage the mesoporous starch is doped with a catalytic amount of an organic acid and oven dried under vaccuum (Scheme 4) [48]. Obtained samples were heated to various carbonization temperatures with different porosities and different types and concentrations of functional groups (Starbon-250, Starbon-400 and Starbon-800) (Scheme 5). Associated with the diversity of surface functional groups Starbon® can be chemically modified relatively easily. Thus, treatment of Starbon® materials with triflic acid can result in solid materials with acidic properties. This was achieved with concentrated triflic acid (10 mL acid g-1 material) and heating at 80 °C for 10h. Subsequently, samples were washed with distilled water to remove residual unadsorbed acid to neutral pH and dried at 80 or 120 °C for 8h.

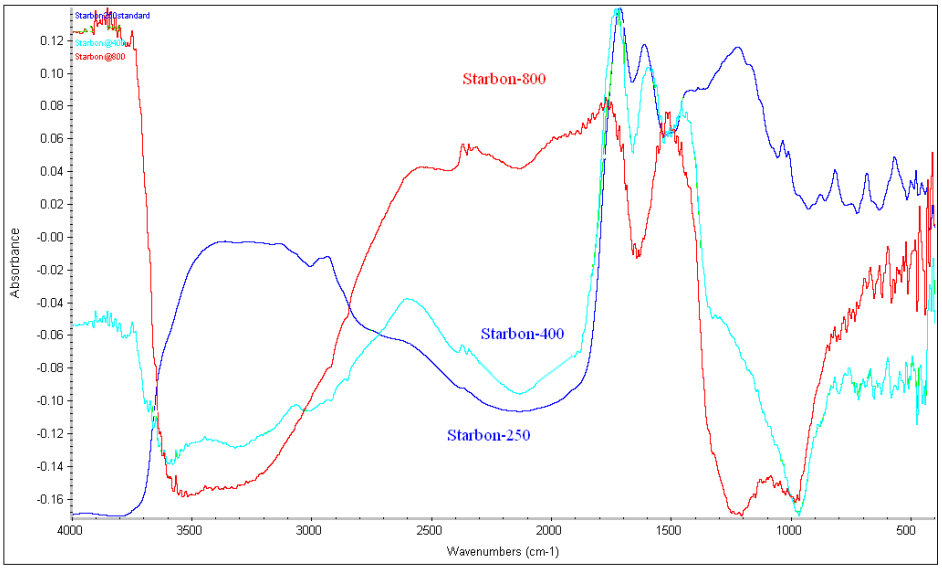

Figure 15. *DRIFT spectra of carbonised Starbon samples at different temperatures.*

The nature and density of the functional groups on the surface of the samples vary with the carbonization temperature. Thus, in the first stept (i.e. 150-200°C), starch backbone-CH_2OH groups condensed to form ether groups, in the second stept at 200-300°C, residual -CH_2OH groups condensed to carbonyl groups conjugated to olefinic groups with the formation of aliphatic and alkenic/aromatic functions. . In the final step, at carbonisation temperatures >300°C, the aliphatic groups are gradually converted to voluminous aromatic systems. DRIFT spectroscopy confirmed these changes, showing a progressive decrease in the concentration of -CH_2OH groups and an increase in aliphatic and aromatic functions (Figure 15). Such changes are similar to those reported in the literature for starch except that in the case of Starbon they occur at much lower temperatures [19]. The triflation of the Starbon-250 sample is evidenced by the appearance of a band at 1530 cm^{-1}, attributed to the SO_3CF_3 group [49].

Such a compositional change in the surface layer explains the progressive decrease in the material ability to retain triflate species. Thus, in the IR spectra a decrease of their characteristic bands (639 cm^{-1} - SO_2CF_3; 761 cm^{-1} S-O; 1030 cm^{-1} S=O) is observed from Starbon 250, to Starbon 400 and Starbon 800, corresponding to a decrease in the population of triflat species (Figure 16).

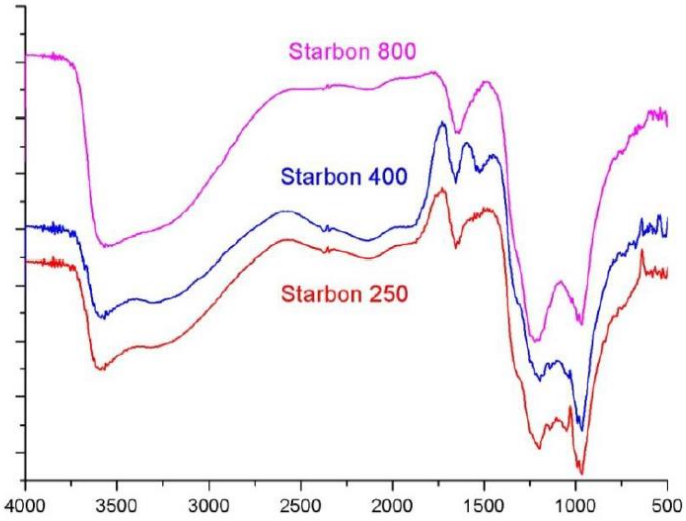

Figure 16. *IR spectra of Starbon samples dried at 150°C and calcined at 250, 400 and 800°C respectively.*

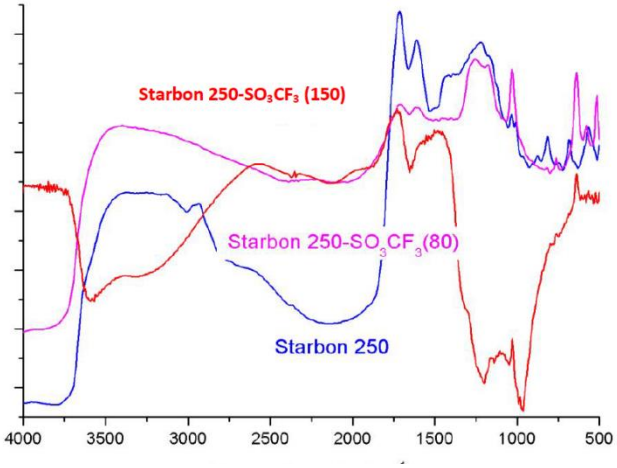

Figure 17. *IR spectra for Starbon 250 sample, treated with triflic acid and dried at 80°C and 150 °C respectively.*

The highest conversions and selectivities were obtained for a sample with a hydrophilic surface (Starbon 250). In contrast, catalysts with hydrophobic surface (Starbon 800) showed low activities and selectivities. These catalysts also showed high hydrothermal stability. Drying is also important influencing the amount of surface retained triflate species as evidenced by IR spectra at temperatures between 80 and 150°C (Figure 17). In the presence of Starbon-250 sample, after 3h of reaction, the glucose conversion was 100% with the following distribution of reaction products: 38.5% levulinic acid, 28.6% formic acid, 23.6% butanoic acid and 9.2% succinic acid. This result is encouraging, especially since few examples of levulinic acid formation at temperatures below 200°C are known in the literature (Figure 18). The DRIFT spectrum of Starbon-250 sample treated with triflic acid highlights the species catalyzing the glucose isomerization reaction (Figure 19:

1031 cm^{-1} -S=O; 1200 cm^{-1}, 1530 cm^{-1} -SO_2CF_3). These catalysts exhibit high hydrothermal stability.

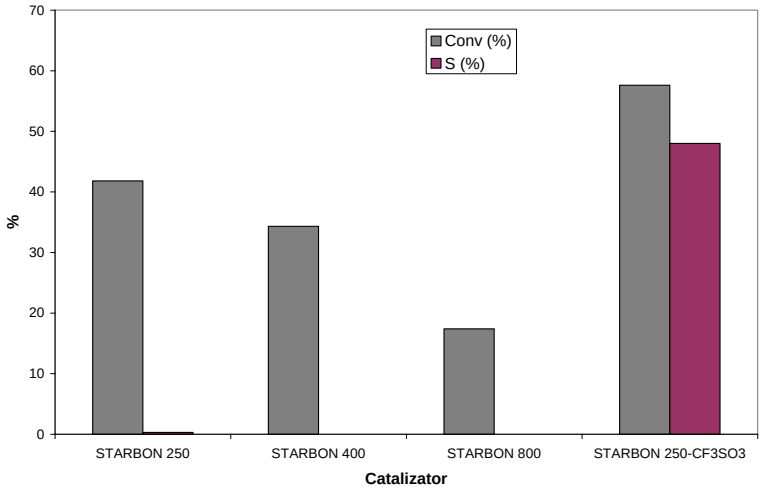

Figure 18. *Variation of cellulose conversion and selectivity in LA in the presence of Starbon type catalysts as such and modified with triflic acid (reaction conditions: cellulose 0.14g, water 5 ml, catalyst 0.06g, T=180°C).*

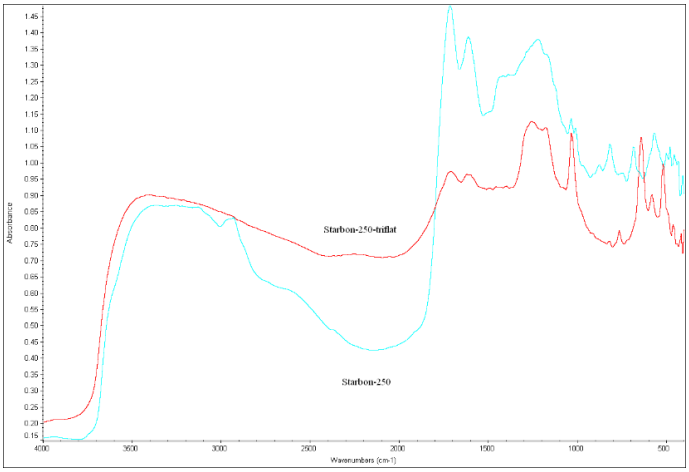

Figure 19. *DRIFT spectra of Starbon-250 and Starbon-250 samples treated with triflic acid.*

General Conclusions

This thesis is on the topic of *Biomass valorization based on green chemistry principles*, aiming at *The design of advanced catalytic systems for the selective valorization of lignocellulosic biomass to bio-chemicals*. In the four experimental chapters original results are presented on: (i) Tin-doped MgF_2 metal fluoride catalysts for fast and selective conversion of cellulose to glucose (Chapter 3), (ii) Direct synthesis of sorbitol and glycerol from cellulose in the presence of magnetic nanoparticle/ionic Ru catalysts in the absence of an external hydrogen source (Chapter 4), iii) Transformation of cellulose to bio-chemicals in the presence of heterogeneous catalysts (Chapter 5), and iv) Catalytic methods for the transformation of marine polysaccharides to monosaccharides

and levulinic acid (Chapter 6). In each of the investigated examples the selected catalysts showed high performance. All catalysts tested were comprehensively characterised using diffractometric and spectroscopic techniques.

All these results are reported in 4 articles published in journals with wide international recognition (Cumulative Impact Factor 20,374). Original results have also been disseminated as oral presentations in 8 high impact international conferences.

Dissemination

I. List of papers

1. Wuttke, S., Negoi, A., Gheorghe, N., Kuncser, V., Kemnitz, E., Parvulescu, V. I., Coman, S. M. (**2012**): Novel Sn-doped hydroxylated MgF_2 catalysts for the fast and selective saccharification of cellulose to glucose, *ChemSusChem*, 5 (9) , 1708-1711 (f.i.= 6.827);
2. Negoi, A., Trotus, I. T., Mamula Steiner, O., Tudorache, M., Kuncser, V., Macovei, D., Parvulescu, V. I., Coman, S. M. (**2013**): Direct synthesis of sorbitol and glycerol from cellulose over ionic Ru-MNP and in the absence of external hydrogen, *ChemSusChem*, 6 (11), 2090-2094 (f.i. = 7.475);
3. Negoi, A., Triantafyllidis, K., Parvulescu, V. I., Coman, S. M. (**2014**): The hydrolytic hydrogenation of cellulose to sorbitol over M (Ru, Ir, Pd, Rh)-BEA-zeolite catalysts, *Catal. Today* 223, 122– 128 (f.i. = 3.464);
4. Podolean, I., Negoi, A., Candu, N., Tudorache, M., Parvulescu, V. I., Coman, S. M. (**2014**): The cellulose capitalization to bio-chemicals in the presence of magnetically nanoparticles catalysts, *Topics Catal*, 57, 1463-1469 (f.i. = 2.608).

II. Contributions to international and national conferences

1. Alina Negoi, Vasile I. Parvulescu, Simona M. Coman, *„The hydrogenolysis of cellulose to sugar alcohols on Me (Me = Rh, Ru, Pd, Ir) / BEA-zeolite catalysts”*, COST Action CM 0903 (UBIOCHEM), 3rd Workshop, November 1-3, **2012**, Thessaloniki, Greece (prezentare orala);
2. S. Wuttke, A. Negoi, N. Candu, N. Gheorghe, V. Kuncser, E. Kemnitz, V. I. Parvulescu, S. M. Coman (**2013**): Fast and selective cellulose saccharification to glucose on Sn-doped hydroxylated MgF_2 catalysts, XIth European Congress on Catalysis (EUROPACAT), Lyon, France, 1-6 September (prezentare orala);
3. N. Candu, A. Negoi, I. Podolean, M. Tudorache, V. I. Parvulescu, S. M. Coman (**2013**): Fine tuning of the magnetically nanoparticles catalysts properties for selective transformation of cellulose to value-added chemicals, The 6th Asia-Pacific Congress on Catalysis (APCAT-6), Taipei, Taiwan, 13-17 October (prezentare orala;

4. Natalia Candu, Iunia Podolean, Alina Negoi, Vasile I. Parvulescu, Simona M. Coman (**2014**): The cellulose capitalization to bio-chemicals in the presence of magnetically nanoparticles catalysts, 25th Organic Reactions Catalysis Society Meeting, Tucson, AZ, USA, March 2-6 (prezentare orala);
5. V. Parvulescu, V. Kuncser, A. Negoi, M. Tudorache, S. M. Coman (**2014**): Magnetite nanoparticles as efficient supports for noble metals in the valorisation of biomass, 59th Annual Magnetism & Magnetic Materials Conference, Honolulu, Hawaii, November 3-7 (prezentare orala);
6. A. Negoi, N. Candu, I. Podolean, M. Tudorache, S. M. Coman, V. I. Parvulescu (**2015**) Efficient valorisation of cellulose to useful chemicals by using ruthenium based magnetic nanoparticles, First Workshop of FP1306 COST Action „LIGNOVAL", Belgrad, Serbia, February, 3-5 (prezentare orala);
7. Alina Negoi, Madalina Tudorache, Simona M. Coman, Maryse Gouygou, Phillipe Serp and Vasile I. Parvulescu (**2016)**- *"Tunable chiral organometallic hybrid nanocatalyst for highly enantioselective hydrogenation of dehydroamino acids"*; Cost Action CM1407 ("Challening organic syntheses inspired by nature-from natural products chemistry to drug discovery"), 2nd Meeting, April 4-5, Madrid, Spain (prezentare orala);
8. Lacramioara Zala, Alina Negoi, Simona Coman, *„Starbons®-SO_2CF_3 catalysts for the cellulose hydrolysis to levulinic acid (LA)*", Sesiunea de Comunicari Stiintifice Studentesti, mai **2012**, Bucuresti, Romania (prezentare orala).

Selective bibliography

1. Y.C. Lin, G. W. Huber, *Energy & Environmental Science*, **2009**, *2*, 68–80;
2. Brian F. Towler, *The Future of Energy,* 1st Edition, Elsevier, **2014**, Chapter 1 - The History and Culture of Energy;
3. *History - Cellulose and Renewable Materials Division*, http://cell.sites.acs.org/history.htm;
4. Jorgensen H, Kristensen JB, Felby C., *Biofuels, Bioprod. Bioref.*, **2007**, 1, 119–134;
5. Kamm, B., Gruber, P.R., Kamm, M., *Biorefineries - Industrial Processes and Products. Status Quo and Future Directions.*, **2006**, Vol. 1, WILEY-VCH Verlag GmbH & Co. KGaA, Weinheim, Germany;
6. Kamm, B., Gruber, P.R., Kamm, M., *Biorefineries - Industrial Processes and Products. Status Quo and Future Directions*, WILEY-VCH Verlag GmbH & Co. KGaA, Weinheim, Germany, **2006**, Vol. 1;
7. Huber, G. W.; Iborra, S.; Corma, A., *Chem. Rev.*, **2006**, 106, 4044-4098;
8. A. Corma, S. Iborra and A. Velty, *Chem. Rev.*, **2007**, 107, 2411–2502;
9. D. M. Alonso, . J. Q. Bond e J. A. Dumesic, *Green Chemistry*, **2010**, 12, 1493-1513;
10. Wang, Y., et al., *Nature Communications*, **2013**, 4 (1), 2141;
11. Albert, J., et al., *Energy & Environmental Science*, **2012**, 5(7), 7956-7962;

12. Nandiwale, K.Y., et al., *ACS Sustainable Chemistry & Engineering*, **2014**, 2(7), 1928-1932;
13. Huang, H., et al., *ACS Catalysis*, **2014**, 4 (7), 2165-2168;
14. Liu, C.-G., et al., *Biotechnology Advances*, **2019**, 37 (3), 491-504;
15. Toor, M., et al., *Chemosphere*, **2020**, 242, 125080;
16. R. Shu, J.Long, Y. Xu, L. Ma, Q. Zhang, T. Wang, C. Wang,Z. Yuan, Q. Wu, *Bioresource Technology*, **2016**, 200, 14–22;
17. A. Toledano, L. Serrano, A. Pineda, A. A. Romero, R. Luque, J.Labidi, *Applied Catalysis B: Environmental*, **2014**, 145, 43 –55;
18. Y.Ye, Y. Zhang, J.Fan, J. Chang, *Bioresource Technology*, **2012**, 118, 648–651;
19. H. Lee, J. Jae, J.-M. Ha, D. J. Suh, *Bioresource Technology*, **2016**, 203, 142–149;
20. B. B. Hallac e . A. J. Ragauskas, Biofuels, *Bioproducts and Biorefining*, **2011**, 5, 215–225;
21. Y.-C. Lin and G. W. Huber, *Energy & Environmental Science*, **2009**, 2, 68-80;
22. Jessica Heigner; Conversion of cellulose into biofuel precursors via solid supported acid catalysis, *ProQuest LLC.*, **2012**, 1,2;
23. Luo C, Wang S, Liu H.; *Angew. Chem. Int. Ed.*, **2007**, 46, 7636;
24. Ji, N., et al., *Catalysis Today*, **2009**, 147 (2), 77-85;
25. Zhang, Y., A. Wang, and T. Zhang, *Chemical Communications*, **2010**, 46 (6), 862-864;
26. A. M. Ruppert, K. Weinberg, and R. Palkovits, *Angewandte Chemie-International Edition*, **2012**, 51(11), 2564–2601;
27. S. Van de Vyer, J. Geboers, P.A. Jacobs, B.F. Sels, *ChemCatChem.*, **2011**, 3, 82-94;
28. Polshettiwar, V.; Tewodros, A., *Nanocatalysis: Synthesis and Applications*, John Wiley & Sons, **2013**;
29. S. Wuttke, S. M. Coman, G. Scholz, H. Kirmse, A. Vimont, M. Daturi, S.L.M. Schroeder, E. Kemnitz, *Chem. Eur. J.*, **2008**, 14, 11488;
30. A. Onda, T. Ochi, K. Yanagisawa, *Green Chem.*, **2008**, 10, 1033 – 1037;
31. V. I. P rvulescu, S. Coman, P. Palade, D. Macovei, C. M. Teodorescu, G. Filoti, R. Molina, G. Poncelet, F. E. Wagner, *Appl. Surf. Sci.*, **1999**, 141, 164 – 176;
32. S. Wuttke, A. Negoi, N. Gheorghe, V. Kuncser, E. Kemnitz, V. I. Parvulescu, S. M. Coman, *ChemSusChem.*, **2012**, 5, 1708 – 1711;
33. H. Kobayashi, T. Komanoya, K. Hara, A. Fukuoka, *ChemSusChem.*, **2010**, 3, 440 – 443;
34. W. Bottcher, G. M. Brown, N. Sutin, *Inorg. Chem.*, **1979**, 18, 1447 – 1451;
35. A. Negoi, K. Teinz, E. Kemnitz, S. Wuttke, V.I. Parvulescu, S.M. Coman, *Topics in Catalysis*, **2012**, 55, 680–687;
36. Y. Nie, G.-K. Chuah, S. Jaenicke, *Chemical Communications*, **2006**, 7, 790–792;
37. F. Iosif, S. Coman, V. Parvulescu, P. Grange, S. Delsarte, D. De Vos, P. Jacobs, *Chemical Communications*, **2004**, 1292–1293;
38. S. Wuttke, A. Negoi, N. Gheorghe, V. Kuncser, E. Kemnitz, V.I. Parvulescu, S.M. Coman, *ChemSusChem*, **2012**, 5 (9), 1708–1711;

39. H. Kobayashi, Y. Ito, T. Komanoya, Y. Hosaka, P.L. Dhepe, K. Kasai, K. Hara, A. Fukuoka, *Green Chemistry*, **2011**, 13, 326–333;
40. V. Jollet, F. Chambon, F. Rataboul, A. Cabiac, C. Pinel, E. Guillon, N. Essayem, *Green Chemistry*, **2009**, 11, 2052–2060;
41. O. Bobleter, *Progress in Polymer Science*, **1994**, 19, 797–841;
42. T. Komanoya, H. Kobayashi, K. Hara, W.-J. Chun, A. Fukuoka, *Applied Catalysis A: General*, **2011**, 407, 188–194;
43. Bobleter O, *Prog. Polym. Sci*., **1994**, 19, 797;
44. Negoi A, Trotus IT, Mamula Steiner O, Tudorache M, Kuncser V, Macovei D, Parvulescu VI, Coman SM, *ChemSusChem*, **2013**, 6, 2090–2094;
45. Q. Xiang, Y. Y. Lee, P. O. Pettersson, R. W. Torget, *Appl. Biochem. and Biotech.*, **2003**, 105-108, 505-514;
46. Bo¨ttcher W, Brown GM, Sutin N, *Inorg. Chem.*, **1979**, 18, 1447;
47. Parvulescu VI, Coman S, Palade P, Macovei D, Teodorescu CM, Filoti G, Molina R, Poncelet G, Wagner FE, *Appl. Surf. Sci.*, **1999**, 141, 164;
48. R. J. White, V. L. Budarin, J. H. Clark, *ChemSusChem*, **2008**, 1, 408;
49. S. M. Coman, M. Florea, V. I. Parvulescu, V. David, A. Medvedovici, D. De Vos, P. A. Jacobs, G. Poncelet, P. Grange, *J. Catal.*, **2007**, 249, 359–369.